JOURNAL OF GEOPHYSICAL RESEARCH, VOL. ???, XXXX, DOI:10.1029/,

Scattering of suprathermal electrons in the solar wind: ACE observations

Christina Pagel

Center for Space Physics, Boston University, Boston, Massachusetts, USA

S. Peter Gary, Curt A. de Koning, Ruth M. Skoug, and John T. Steinberg

Los Alamos National Laboratory, Los Alamos, New Mexico

C. Pagel, Clinical Operational Research Unit, University College London, 4 Taviton Street, London, United Kingdom WC1H0BT cpagel@ucl.ac.uk

S. P. Gary, R. M. Skoug, and J. T. Steinberg, Group ISR-1, Los Alamos National Laboratory, Los Alamos, NM 87545, USA

C. A. de Koning, NOAA Space Environment Center, Boulder, CO 80305, USA

Abstract. Suprathermal electrons in the solar wind have a strahl component with velocity distributions which are narrow in pitch-angle and are directed along the background magnetic field away from the Sun. Analysis of strahl distributions from 73.3 eV to 987 eV as measured during the year 2004 by the SWEPAM plasma instrument on the ACE spacecraft are reported here. Although most previous observations show that the strahl pitch-angle width decreases with increasing energy, this manuscript describes 29 scattering events observed at times of enhanced, relatively high-frequency magnetic fluctuations which show that this width increases as strahl energy increases. This manuscript also develops the hypothesis that this characteristic is due to electron scattering by background whistler fluctuations.

1. Introduction

Solar wind electrons near 1 AU are characterized by two distinct populations, a thermal ($\sim$ 10 eV), relatively dense core (denoted by subscript c) and a more tenuous suprathermal (80 eV to more than 1 keV) component (subscript s). The original interpretation of the suprathermals was that they could be represented as a single velocity distribution [*Feldman et al.*, 1975]. Subsequent analyses [*Rosenbauer et al.*, 1977; *Feldman et al.*, 1978] showed that the suprathermals usually consist of two distinct components, a relatively isotropic halo and a highly anisotropic, narrow magnetic-field-aligned "strahl" (For detailed bibliographies on suprathermal electron observations, see *Marsch* [1991] and *Pagel et al.* [2005]). The flows of these three components relative to the ions satisfy the zero current condition but correspond to a non-zero heat flux $\mathbf{q}_e$ directed away from the Sun and parallel or antiparallel to the interplanetary magnetic field $\mathbf{B}_o$.

The narrow strahl has been used to probe properties of the solar wind at distances remote from the observing spacecraft. Under the assumption that these suprathermals propagate relatively scatter-free from their source, *Gosling et al.* [2001, 2002, 2005] deduced large-scale properties of the interplanetary magnetic field, and *Gosling et al.* [2003, 2004] inferred properties of the coronal source regions for suprathermal electron bursts. Because the scatter-free assumption is an important element in the logical process leading to the conclusions of these papers, it is important to critically examine how suprathermal electrons may be scattered in the solar wind, and to attempt to understand the conditions that lead to such scattering. This manuscript addresses this question, describing a study

of strahl observations from the ACE spacecraft which show a likely signature of whistler scattering.

If interplanetary plasma were strictly collisionless, conservation of the first adiabatic invariant would lead to a reduction of the perpendicular speeds of all charged particles as the solar wind flows away from the Sun and B_o decreases. This implies the global development of $T_\perp/T_\parallel < 1$ electron anisotropies where the directional subscripts correspond to directions relative to the average or background magnetic field $\mathbf{B}_o$ [e.g., *Phillips and Gosling* [1990]]. The narrow, anti-Sunward strahl is apparently a manifestation of this focusing *Ogilvie et al.* [2000], and is a primary contributor to the electron heat flux [*Feldman et al.*, 1975; *Scime et al.*, 1994].

Particle-particle collisions are most effective in dense, cool plasmas, and are usually credited with keeping the core relatively isotropic [*Phillips and Gosling*, 1990], although at times the core may also exhibit a strong $T_\perp/T_\parallel < 1$ [*Phillips et al.*, 1989]. *Salem et al.* [2003] studied the role of Coulomb collisions on solar wind electrons at 1 AU and concluded that such collisions help constrain both the electron temperature anisotropy and the electron heat flux, especially in plasmas with relatively short electron mean free paths. The mean free paths of relatively hot particles increase as the square of the energy, so that particle-particle collisions are not very effective for suprathermal electrons, providing a plausible explanation for observations of strahl widths which decrease with increasing energy [e.g., *Feldman et al.* [1978], *Pillip et al.* [1987a]]. *Pillip et al.* [1987b] conclude that Coulomb collisions cannot be the mechanism which leads to the nearly isotropic suprathermal distributions observed at solar wind sector boundaries by the Helios spacecraft, and unspecified pitch-angle scattering mechanisms are often invoked to explain

the relative isotropy of the halo (e.g. *Gosling et al.* [2001]). The strahl is not as narrow as exospheric (i.e. collisionless) models predict, but particle-particle scattering apparently cannot describe the observed widths of this component [*Lemons and Feldman*, 1983].

Wave-particle interactions are an alternative mechanism to scatter suprathermals and specifically to reduce strahl anisotropies. There are at least two likely sources of such scattering. Electrostatic waves at $\mathbf{k} \times \mathbf{B_0} = 0$, especially enhanced fluctuations driven by electron/electron instabilities, can slow the parallel velocities of suprathermals without affecting $v_\perp$; in effect, this leads to an increase in pitch angles. A more direct source of electron pitch-angle scattering is electromagnetic fluctuations at propagation approximately parallel to $\mathbf{B}_o$.

At sufficiently small amplitudes, electromagnetic fluctuations may be categorized either as Alfvén-cyclotron waves, with left-hand polarization, $\omega_r < \Omega_p$, and $k_\| c/\omega_p < 1$, or magnetosonic-whistler waves with right-hand polarization, $\omega_r < |\Omega_e|$, and $k_\| c/\omega_e < 1$ [e.g., see Chapter 6 of *Gary,* [1993]] (See the Appendix for definitions of symbols.). Cyclotron wave-particle interactions are strongest when the parallel velocity, $v_\|$, of a jth species particle satisfies the cyclotron resonance condition

$$k_\| v_\| = \omega_r \pm \Omega_j \ . \tag{1}$$

For the modest β_e values typical of the solar wind, all Alfvén-cyclotron fluctuations and lightly damped whistlers satisfy $|\omega_r| << |\Omega_e|$, so that the electron resonance condition for both categories of fluctuations may be written as

$$\frac{1}{2} m_e v_\|^2 = \frac{1}{2} m_p v_A^2 (\frac{\omega_e}{k_\| c})^2 \tag{2}$$

or, using typical solar wind values of $n_e = 5$ cm^{-3} and $B_o = 5$ nT,

$$\frac{1}{2} m_e v_{\|}^2 = (12.4eV) \left(\frac{\omega_e}{k_{\|} c} \right)^2 \tag{3}$$

Thus, suprathermal electrons between 100 eV and 1 keV are on average resonant with wavenumbers $0.10 \lesssim k_{\|} c/\omega_e \lesssim 0.35$, corresponding to whistler fluctuations.

Figure 1 illustrates the suprathermal electron cyclotron resonance corresponding to representative solar wind parameters near 1 AU. Suprathermals with $v_{\|} > 0$ resonate with whistler fluctuations at $\omega_r/k_{\|} < 0$; the two cyclotron resonant speeds shown here correspond to $k_{\|} c/\omega_e = 0.20$ and 0.40, which approximately bound the domain of significant suprathermal damping. *Vocks and Mann* [2003] and *Vocks et al.* [2005] developed a solar wind electron model to show that scattering by whistler fluctuations could lead to broadened strahl similar to those observed from the WIND spacecraft.

Although the isotropic character of the halo clearly indicates strong wave interactions with suprathermal electrons, there is relatively little observational evidence linking this property to specific scattering mechanisms. *Pillip et al.* [1987b] observed that suprathermal electron distributions become nearly isotropic at solar wind sector boundaries, but, after excluding Coulomb collisions as the isotropization source, could not identify an alternative mechanism to produce this result. Two studies of "magnetic holes" in the solar wind showed that suprathermal electron velocity distributions became quite isotropic within these regions of substantially reduced $|\mathbf{B}_o|$. *Chisham et al.* [2000] observed no increase in the level of electric field fluctuations at $f > 100$ Hz in the two magnetic depressions they studied, whereas *Zurbuchen et al.* [2001] noted a consistent increase in the $|\delta B|^2/B_o^2$ in many of their magnetic holes. *Crooker et al.* [2003] carried out a statistical analysis on more than six years of observations from the Wind spacecraft to show a strong

inverse correlation between the suprathermal electron anisotropy and the plasma β in the solar wind. This anticorrelation led *Crooker et al.* [2003] to conclude that the high-β solar wind is conducive to electron pitch-angle scattering. This result is suggestive of the β_e dependent electron anisotropy constraint imposed by the whistler anisotropy instability [*Gary and Wang*, 1996] which has been observed in the magnetosheath *Gary et al.* [2005]. Recently *de Koning et al.* [2006] analyzed pitch-angle distributions of suprathermal solar electron bursts and found that 60% of these bursts had broader beams than the preceding strahl. They concluded that broadening of the pitch-angle distributions during such bursts most likely results from wave-particle scattering.

Most observations to date have shown that the strahl becomes more anisotropic [*Feldman et al.*, 1978; *Pillip et al.*, 1987a; *Ogilvie et al.*, 2000] or retains the same anisotropy [*Hammond et al.*, 1996] as electron energy increases. However, recent fast wind observations of *Pagel et al.* [2005] show that the strahl becomes broader in pitch-angle with increasing electron energy. This manuscript describes our research efforts to characterize this uncommon property and to better understand the physical processes which cause it.

Section 2 describes our ACE/SWEPAM measurement studies. Section 3 develops our hypothesis that scattering by background whistler fluctuations is a source of electron strahl pitch-angle distributions which become broader in pitch-angle as electron energy increases. Section 4 summarizes our results and conclusions.

2. Observations

In this section, we use ACE/SWEPAM measurements to study electron strahl observed in 29 scattering events at times of enhanced, relatively high-frequency magnetic fluctuations.

2.1. Data

We use one minute resolution suprathermal electron and plasma data from the SWEPAM instrument [*McComas et al.*, 1998] and magnetic field data from the MAG instrument [*Smith et al.*, 1998] on the ACE spacecraft. Quasilinear theory predicts that particle scattering rates are proportional to the square of the fluctuating field amplitudes, so we look for events with high $|\delta B|/B_o$ where we might see such scattering in the suprathermal electrons.

To characterize the level of magnetic fluctuations, we use δB_{rms} as calculated by *Smith et al.* [2001]. This quantity is calculated from MAG instrument data as the RMS vector fluctuation computed every 16 s using 3 vector/s measurements. Given that the a typical proton cyclotron frequency in the solar wind near 1 AU is about 0.1 Hz [*Leamon et al.*, 1998], the 3 Hz sampling of δB_{rms} implies that this parameter represents the low-frequency whistler regime. The $|\delta B|/B_o$ is higher when B_o is low or when background fluctuations are high (or both). These conditions are more likely to be met in the quieter fast ambient solar wind, and are consistent with the studies of *Chisham et al.* [2000], *Zurbuchen et al.* [2001] and *Pagel et al.* [2005]. The ACE spacecraft was launched in 1998, during the rising phase of the solar cycle, so to maximise the amount of ambient fast wind we use data from 2004 in this study. Before detailing the results of our survey we need to introduce one of the key electron parameters we use to select events and to analyse them.

2.2. Electron Parameters

This subsection describes our paramerization of strahl structure in such a way as to quantify its response to scattering. A traditional method for describing the width of the strahl distribution is to calculate either a full or half width at half maximum (HWHM)

of the pitch angle distributions [*Hammond et al.*, 1996; *Ogilvie et al.*, 1999, 2000; *de Koning et al.*, 2006]. This is a measure of the angular width of the strahl. However, the method of obtaining the HWHM by fitting a Gaussian to the pitch angle distribution typically introduces uncertainty in the final value. Certainly, when there is some counter-streaming or a near-isotropic pitch angle distribution, fitting a Gaussian is problematic and the resulting HWHM values can be unreliable. While *Hammond et al.* [1996] and *Ogilvie et al.* [1999] circumvent these problems by only considering strahls where there is a clear narrow beam, more complete studies of suprathermal electron scattering should involve both broader strahls and even isotropic pitch angle distributions. Thus we suggest that a more robust parameterisation of the electron pitch angle distributions is needed.

Pagel et al. [2005] used a log variance measure of the pitch angle distributions, based on normalised pitch angle fluxes. This parameter is simplistic but reasonably robust, particularly when trying to parameterise a pitch angle distribution with relatively few pitch angle bins. We here introduce a different, and we believe better, parameter: the absolute value of the skew of the pitch angle distribution between 0^o and 180^o. The skew of the pitch angle distribution is dimensionless and defined as the third moment of a distribution normalised by its standard deviation:

$$Skew = \frac{(\sum_i (x_i - \overline{x})^3)/N}{\sigma^3} \tag{4}$$

where x_i are the flux counts in each pitch angle bin i and σ is their standard deviation. The skew is a measure of a distribution's asymmetry. Its sign indicates whether a distribution is skewed to the left (negative) or to the right (positive) of the mean. Since pitch angle distributions can be skewed in either direction depending on the direction of the magnetic field and we care only about the amount of asymmetry, we use simply the absolute value

of the skew in this study. A skew of zero corresponds to a totally symmetric distribution; in the case of a pitch angle distribution between 0^o and 180^o this would correspond, for example, to a fully isotropic distribution or to two identical counterstreaming electron beams. A narrow, unidirectional strahl gives a relatively high value for the skew (~ 3). If an instrument provides only a few pitch angle bins, skewness can be a noisy measure because of the influence of extreme points on its value. Also, if there are significant counter-streaming electron beams (or 90^o pitch angle depletions [*Gosling et al.*, 2001]) the skew is not a useful measure of strahl width. However, given a sufficient number of pitch angle bins and little or no counter-streaming, the skew has several advantages over HWHM measures: it is very quick to calculate, does not rely on any fitting process and does not lose its reliability as pitch angle distributions approach isotropy. High skews and low HWHM values both correspond to narrow strahls, so these two parameters are anticorrelated. Thus, we use inverse skewness as a proxy for strahl width.

An example of how both skew and HWHM parameterise the strahl is given in Figure 2. The top panel shows the colour-coded pitch angle distribution for $E = 272$ eV, where the yellow-red band parallel to the magnetic field signifies the strahl. The colour represents the log of the flux counts in each pitch angle bin. It is clear from panel (a) that the strahl width is variable and it is some of this variation that we are attempting to explain in this manuscript. Panels (b) and (c) give the corresponding skew and HWHM of the pitch angle distributions respectively. They are anti-correlated, as expected, since broad strahls correspond to smaller skews and larger angular widths. Panels (d) and (e) give the magnetic field strength and $|\delta B|/B_o$ respectively. Comparison of panels (a), (b) and (e) show some correlation between peaks in $|\delta B|/B_o$ and broadening of the strahl.

Figure 3 makes explicit the relationship between skew and HWHM in a scatter plot. The blue circles represent the values of each of these quantities from the same time period as Figure 2, while the red dots are from another day and a half in 2004 as a consistency check. Both times are within unidirectional suprathermal electron periods. Given the excellent correlation between them, we feel confident that skew can be used as an accurate proxy for strahl angular width. We shall use this parameter to investigate the property of electron scattering in regions of high $|\delta B|/B_o$.

2.3. Results

Quasilinear theories predict, and we expect, that magnetic fluctuations scatter electrons more strongly when $|\delta B|/B_o$ is relatively large. Thus we first select times in 2004 where $|\delta B|/B_o > 0.15$. To remove spikes and to ensure a sufficient amount of data during an event, we further require that $|\delta B|/B_o > 0.15$ for at least ten minutes. We examine the remaining high $|\delta B|/B_o$ events by eye using electrons at 519 eV. If the strahl is disordered, if there is counter-streaming or if there is no change in the skew we reject the event. If there is a clear drop in skew during the high $|\delta B|/B_o$ event, but no visible change in the strahl, we check the individual pitch angle distributions through the event. If a broadening of the distributions in pitch angle is evident from these, the event is kept, otherwise it is rejected. We note that this process explicitly allows for the fact that there is not a one-to-one correspondence between high $|\delta B|/B_o$ and pitch angle scattering. Figure 4 shows an example event from our survey delineated with the red and blue lines. Although the scattering is not extreme, the strahl does broaden and the skew does drop during this event.

We find a total of 29 events in 2004, ranging from 14 to 38 minutes in duration, with a mean of 23 minutes. In general, plasma parameters such as solar wind speed, density and temperature are steady for these times. For each of these events we examine strahl characteristics with energy from 73 eV to 987 eV. Figure 5 shows an example event from the survey. We average the pitch angle distributions for each energy over the event (which lasted for 19 minutes), and then normalise the fluxes for each energy the value at 158 degrees (in the non field aligned direction). By plotting the resulting normalised distributions together we can qualitatively compare their scattering characteristics. It is clear that as electron energy increases, the pitch angle distributions become broader. This implies that the strahl over this event is scattered most at the highest energies, counter to what is normally observed. To consider the scattering behaviour with energy for all our events, we use skew to quantify scattering.

Since skew is inversely proportional to strahl width, the minimum value of the skew at each energy corresponds to the maximum strahl width at that energy during the event. We will use minimum skew for each energy to investigate the energy dependence of scattering. The same example event illustrated in Figure 5 is shown by the black line in figure 6, which clearly shows skew decreasing with energy. The composite behaviour of all 29 scattering events is given by the red line, which shows the same trend. Given the inverse relationship between skew and HWHM, these results demonstrate that, for each of these events of enhanced magnetic fluctuations, the strahl broadens with increasing energy.

For each data point during the 29 events (a total of 626 points), we calculate the energy at which the strahl is most skewed (i.e. has the narrowest width). Figure 7 gives the distribution of these energies for all data points in our events. Note that we have limited

our calculations to E >100eV to avoid any possible contamination from the core. As is clear from the histogram, the lowest energies most often have the narrowest strahls which further establishes the behaviour seen in figure 6. Such an energy dependence of strahl width during periods of high magnetic field fluctuations has not been reported before.

To model wave-particle interactions, we need a functional form for the strahl parallel energy distribution $f_s(E)$. To obtain such a form we considered distributions at velocities most closely aligned with the magnetic field, and carried out fits to twelve different samples from our data set. Figure 8 shows a result representative of all these samples: the fit to an exponential in energy (i.e., a Maxwellian velocity distribution) is relatively poor, whereas the fit to a power law in energy (dashed line) is relatively better but is still unsatisfactory.

Suprathermal electrons in the solar wind are observed to display characteristics of both power-law [*Maksimovic et al.*, 1997] and Maxwellian-like (*Lin,* [1998], *Ogilvie et al.* [2000]) distributions. Thus we assume a product of a power law and an exponential:

$$f_s(E) = \alpha E^{-\gamma} exp(-\beta E) \tag{5}$$

Of course the three-parameter fit of Equation 5, provides a better fit than the two-parameter fits of either a power law or an exponential alone. Nevertheless, Figure 8 shows that the fit to Equation 5 is much more satisfactory, suggesting that this equation should represent a good starting point for theoretical and computational models for wave-particle scattering of the strahl.

We note here that in the days surrounding our events the ambient solar wind strahl can also display such an energy dependence - that is the broadest strahls are at the highest energies. A preliminary analysis of these strahls suggests that they exhibit higher levels

of fluctuations than those times when the strahl is narrower at higher energies. This is consistent with the idea that in regions of enhanced magnetic field fluctuations, whistler waves can scatter electrons. However, a much broader, more detailed study needs to be done to quantify the frequency of such 'anomalous' strahls in the solar wind and is beyond the scope of this manuscript.

3. Scattering of Suprathermal Electrons: Possible Mechanisms

As Figure 1 shows, the plasma fluctuations most likely to provide cyclotron resonant scattering of suprathermal electrons in the solar wind are in the whistler mode. Relatively steady whistler-like fluctuations have been observed from many solar wind spacecraft including Helios 1 and 2 [*Beinroth and Neubauer* [1981]; *Gurnett,* [1991], and references therein], Ulysses [*Lengyel-Frey et al.*, 1996], and Cluster [*Bale et al.*, 2005]. Furthermore, bursty enhanced whistlers have also been measured in the interplanetary medium [*Kennel et al.*, 1980; *Coroniti et al.*, 1982; *Lin et al.*, 1998].

One possible source of bursty whistler fluctuations in the solar wind is electromagnetic instabilities. *Gary et al.* [1999a, b] used the theory of the whistler heat flux instability [*Gary et al.* [1975]], based on a bi-Maxwellian halo and core electron model and driven by the halo/core relative speed, to interpret electron observations from the ACE spacecraft. However, *Scime et al.* [2001] found no correlation between the scaled electron heat flux and whistler-frequency fluctuations observed by Ulysses, concluding that the whistler heat flux instability does not play an important role in limiting the solar wind heat flux. This conclusion has been reinforced by unpublished computer simulations which show that the whistler heat flux instability saturates at very low amplitudes and does not yield a clear signature of electron scattering. As stated above, a more realistic model of suprathermal

electrons is that they consist of an isotropic halo plus a highly anisotropic strahl, with the latter component carrying the heat flux. This model suggests that a firehose type instability based on $T_{\|} >> T_{\perp}$ might be a source of suprathermal electron scattering, and more specifically of anisotropy reduction on the strahl [*Paesold and Benz*, 1999; *Li and Habbal,*, 2000; *Messmer*, 2002; *Gary and Nishimura* , 2003]. However, firehose instabilities based on bi-Maxwellian velocity distributions require the $\beta_{\|}$ of the anisotropic component to be greater than unity, a condition which is rarely satisfied by the tenuous strahl. In the absence of a clear mechanism to provide unstable whistler fluctuations, we conclude that instabilities are not a likely source of suprathermal electron scattering.

A second possible source of suprathermal scattering is the quasi-steady background whistler fluctuations in the solar wind. Figure 9 is a cartoon representing our interpretation of typical solar wind magnetic fluctuation power spectra. At the longest wavelengths, $|\delta B|^2/B_o^2$ is sufficiently large that nonlinear processes dominate and the ensemble of fluctuations must be described by theories of strong turbulence. As k increases, magnetic power spectra decrease approximately as $k^{-5/3}$, so that, at sufficiently short wavelengths, quasilinear and linear theories become valid approximations for describing the fluctuations and we may speak of Alfvén-cyclotron and magnetosonic-whistler modes as recognizable entities.

Near $k_{\|}c/\omega_p \sim 1$ there is a sudden onset of proton cyclotron damping of Alfvén-cyclotron fluctuations [*Gary*, 1999], which rapidly quenches the Alfvénic part of the spectrum, leaving magnetosonic-whistler fluctuations to persist at still shorter wavelengths. *Stawicki et al.* [2001] proposed that the steeper power laws observed $k_{\|}c/\omega_p > 1$ correspond not to strongly damped Alfven-cyclotron fluctuations, but to lightly damped, dispersive whistler

fluctuations, and offered the appellation "dispersion range" for this wavenumber domain. Solar wind magnetic power spectra in this frequency range often correspond to $\sim k^{-3.5}$ (*Beinroth and Neubauer* [1981], *Lengyel-Frey et al.* [1996]), although other observations suggest even steeper power law spectra (*Lin,* [1998], *Leamon et al.* [1998]). At still shorter wavelengths, the onset of electron cyclotron damping should terminate the dispersion range; near $\beta_e \sim 1$ the transition to the electron dissipation range takes place at $k_{||}c/\omega_e \simeq 1$ *Stawicki et al.* [2001].

The Alfvén-cyclotron condition $k_{||}c/\omega_p < 1$ predicts, via Equation 1, that near 1 AU such fluctuations resonantly scatter only those electrons with parallel kinetic energies greater than about 20 keV. This prediction may well be the explanation for the observations of *Lin et al.* [1981] which show significant broadening of fast electron pitch-angle distributions at electron energies greater than about 20 keV [See also the discussion in *de Koning et al.* [2006]]. Similarly, the magnetic fluctuations reported by *Zurbuchen et al.* [2001](see above) correspond to $kc/\omega_p < 1$; by Equation 1 such fluctuations may scatter electrons at greater than 20 keV, but are not likely to strongly affect the 272 eV electrons presented in that paper. Inasmuch as the Alfvén speed v_A increases as distance to the Sun decreases, suprathermal electrons are not likely to be strongly scattered by such fluctuations anywhere in the solar wind between the Sun and the Earth.

In contrast, the whistler condition $\omega_p/c < k_{||} < c/\omega_e$ indicates that both thermal and suprathermal electrons may be scattered by such fluctuations near the Earth, and that even as v_A increases toward the Sun, suprathermal electrons may remain in cyclotron resonance with such waves. Magnetic power spectra usually increase with decreasing wavenumber in the solar wind (Figure 9), corresponding to cyclotron resonance with

faster electrons (Figure 1). Thus the increased suprathermal electron scattering observed at increasing energies is likely due to enhanced scattering by background whistler fluctuations. [*Vocks and Mann* , 2003; *Vocks et al.* , 2005] have demonstrated that background whistlers can indeed pitch-angle scatter the suprathermals; the obvious next step is to use models or simulations to address the energy dependence of that scattering.

4. Conclusions

We have used ACE/SWEPAM observations during the year 2004 to study 29 suprathermal electron scattering events in the solar wind corresponding to enhanced, relatively high-frequency magnetic fluctuations. Our study of the velocity distributions observed during these events in the energy range from 102 eV to 987 eV showed that the pitch-angle width of the strahl electron component uniformly increased as the electron energy increased. We also examined the strahl parallel energy distributions in this energy range and found that a product of power law and exponential factors in energy yielded better fits than either factor alone.

Our experimental results are consistent with the hypothesis developed in Section 3 that this characteristic pitch-angle broadening is due to suprathermal electron scattering by background whistler fluctuations. Further studies will be necessary to test this hypothesis. On the theoretical side, particle-in-cell simulations would be the optimal technique to examine the details of such wave-particle interactions. Further observational studies should examine the statistical relationship between enhanced magnetic power spectra in the whistler range and strahl distributions which exhibit this unusual property. We note that measurements of magnetic power spectra spanning the full range of whistler frequencies are not available from the ACE spacecraft.

5. Appendix: Definitions

We use subscripts $\|$ and $\perp$ to denote directions relative to the background magnetic field $\mathbf{B}_o$. The species subscripts are p for protons, and e for electrons. For the jth species we define $\beta_{\|j} \equiv 8\pi n_j k_B T_{\|j}/B_o^2$; $\tilde{\beta}_{\|j} \equiv 8\pi n_e k_B T_{\|j}/B_o^2 = (n_e/n_j)\beta_{\|j}$; the plasma frequency based on the total electron density, $\omega_j \equiv \sqrt{4\pi n_e e_j^2/m_j}$; the cyclotron frequency, $\Omega_j \equiv e_j B_o/m_j c$; the thermal speed, $v_j \equiv \sqrt{k_B T_{\|j}/m_j}$; and the average flow velocity $\mathbf{v}_{oj}$. We define the Alfvén speed as $v_A \equiv B_o/\sqrt{4\pi n_e m_p}$. The complex frequency is $\omega = \omega_r + i\gamma$, the Landau resonance factor of the jth species is $\zeta_j \equiv \omega/\sqrt{2}|k_\||v_j$, and the cyclotron resonance factors of the jth species are $\zeta_j^\pm \equiv (\omega \pm \Omega_j)/\sqrt{2}|k_\||v_j$.

Acknowledgments. We acknowledge useful conversations with Joe Borovsky and Jack Gosling. The Los Alamos portion of this work was performed under the auspices of the U.S. Department of Energy (DOE) and was supported by the DOE Office of Basic Energy Sciences, Division of Engineering and Geosciences, and the Sun-Earth Connections Theory Program of the National Aeronautics and Space Administration. C. Pagel was supported by the National Science Foundation under grant number ATM-0327739.

References

Bale, S. D., P. J. Kellogg, F. S. Mozer, T. S. Horbury, and H. Reme (2005), Measurement of the electric fluctuation spectrum of magnetohydrodynamic turbulence, *Phys. Rev. Lett., 94*, 215002.

Beinroth, H. J., and F. M. Neubauer (1981), Properties of whistler mode waves between 0.3 and 1.0 AU from Helios observations, *J. Geophys. Res., 86*, 7755.

Chisham, G., S.J. Schwartz, D. Burgess, S.D. Bale, M.W. Dunlop and C.T. Russell, (2000) Multisatellite observations of large magnetic depressions in the solar wind, *J. Geophys. Res.*, *105(A2)*, 2325-2335.

Coroniti, F. V., C. F. Kennel, F. L. Scarf, and E. J. Smith (1982), Whistler mode turbulence in the disturbed solar wind, *J. Geophys. Res., 87*, 6029.

Crooker, N. U., D. E. Larson, S. W. Kahler, S. M. Lamassa, and H. E. Spence (2003), Suprathermal electron isotropy in high-beta plasma and its role in heat flux dropouts, *Geophys. Res. Lett., 30*, 1619, doi:10.1029/2003GL017036.

de Koning, C. A., J. T. Gosling, R. M. Skoug, and J. T. Steinberg (2006), Widths of suprathermal pitch-angle distributions during solar electron bursts: ACE observations, *J. Geophys. Res., , 111*, A04101, doi:10.1029/2005JA011326.

Feldman, W. C., J. R. Asbridge, S. J. Bame, M. D. Montgomery, and S. P. Gary (1975), Solar wind electrons, *J. Geophys. Res., 80*, 4181.

Feldman, W. C., J. R. Asbridge, S. J. Bame, J. T. Gosling, and D. S. Lemons (1978), Characteristic electron variations across simple high-speed solar wind streams, *J. Geophys. Res., 83*, 5285.

Gary, S. P. (1993), *Theory of Space Plasma Microinstabilities*, Cambridge Univ. Press, New York, 1993.

Gary, S. P. (1999), Collisionless dissipation wavenumber: Linear theory, *J. Geophys. Res., 104*, 6759.

Gary, S. P., and J. Wang (1996), Whistler instability: electron anisotropy upper bound, *J. Geophys. Res., 101*, 10,749.

Gary, S. P., and K. Nishimura (2003), Resonant electron firehose instability: Particle-in-cell simulations, *Phys. Plasmas*, *10*, 3571.

Gary S. P., W. C. Feldman, D. W. Forslund, and M. D. Montgomery (1975), Heat flux instabilities in the solar wind, *J. Geophys. Res.,* *80*, 4197.

Gary, S. P., Skoug, R. M., and Daughton, W. (1999a), Electron heat flux constraints in the solar wind, *Phys. Plasmas*, *6*, 2607.

Gary, S. P., Neagu, E., Skoug, R. M., and Goldstein, B. E. (1999b), Solar wind electrons: Parametric constraints, *J. Geophys. Res.,* *104*, 19,843.

Gary, S. P., B. Lavraud, M. F. Thomsen, B. Lefebvre, and S. J. Schwartz (2005), Electron anisotropy constraint in the magnetosheath: Cluster observations, *Geophys. Res. Lett.,* *32*, L13109.

Gosling, J. T., R. M. Skoug, and W. C. Feldman (2001), Solar wind electron halo depletions at 90^o pitch angle, *Geophys. Res. Lett., 28*, 4155.

Gosling, J. T., R. M. Skoug, W. C. Feldman, and D. J. McComas (2002), Symmetric suprathermal electron depletions on closed field lines in the solar wind, *Geophys. Res. Lett., 29*, 1573, doi:10.1029/2001GL013949.

Gosling, J. T., R. M. Skoug, and D. J. McComas (2003), Solar electron bursts at very low energies: Evidence for acceleration in the high corona?, *Geophys. Res. Lett., 30*, 1697, doi:10.1029/2003GL017079.

Gosling, J. T., C. A. de Koning, R. M. Skoug, J. T. Steinberg, and D. J. McComas (2004), Dispersionless modulations in low-energy solar electron bursts and discontinuous changes in the solar wind electron strahl, *J. Geophys. Res., 109*, A05102, doi:10.1029/2003JA010338.

Gosling, J. T., R. M. Skoug, D. J. McComas, and C. W. Smith (2005), Magnetic disconnection from the Sun: Observations of a reconnection exhaust in the solar wind at the heliospheric current sheet, *Geophys. Res. Lett., 32*, L05105, doi:10.1029/2005G:022406.

Gurnett, D. A. (1991), "Waves and Instabilities" in *Physics of the Inner Heliosphere II*, R. Schwenn and E. Marsch, Eds., Springer-Verlag, Berlin.

Hammond, C. M., W. C. Feldman, D. J. McComas, J. L. Phillips, and R. J. Forsyth (1996), Variation of electron-strahl width in the high-speed solar wind: Ulysses observations, *Astron. Astrophys.*, *316*, 350.

Kennel, C. F., F. L. Scarf, F. V. Coroniti, R. W. Fredricks, D. A. Gurnett, and E. J. Smith (1980), Correlated whistler and electron plasma oscillation bursts detected on ISEE-3, *Geophys. Res. Lett., 7*, 129.

Leamon, R. J., C. W. Smith, N. F. Ness, W. H. Matthaeus, and H. K. Wong (1998), Observational constraints on the dynamics of the interplanetary magnetic field dissipation range, *J. Geophys. Res., 103*, 4775.

Lemons, D. S., and W. C. Feldman (1983), Collisional modification to the exospheric theory of solar wind halo electron pitch angle distributions, *J. Geophys. Res., 88*, 6881.

Lengyel-Frey, D., Hess, R. A., MacDowall, R. J., Stone, R. G., Lin, N., Balogh, A., and Forsyth, R. (1996), Ulysses observations of whistler waves at interplanetary shocks and in the solar wind, *J. Geophys. Res., 101*, 27,555.

Li, X., and S. R. Habbal (2000), Electron kinetic firehose instability, *J. Geophys. Res., 105*, 27,377.

Lin, R. P. (1998), WIND observations of suprathermal electrons in the interplanetary medium, *Space Sci. Revs.*, *86*, 61.

Lin, N., Kellogg, P. J., MacDowall, R. J., Scime, E. E., Balogh, A., Forsyth, R. J., McComas, D. J., and Phillips, J. L. (1998), Very low frequency waves in the heliosphere: Ulysses observations, *J. Geophys. Res., 103*, 12,023.

Lin, R. P., D. W. Potter, D. A. Gurnett, and F. L. Scarf (1981), Energetic electrons and plasma waves associated with a solar type III radio burst, *Astrophys. J., 251*, 364.

Maksimovic, M., V. Pierrard, and P. Riley (1997), Ulysses electron distributions fitted with Kappa functions, *Geophys. Res. Lett., 24*, 1151.

Marsch, E., Kinetic physics of the solar wind plasma (1991), in *Physics of the Inner Heliosphere, II, Particles, Waves and Turbulence*, edited by R. Schwenn and E. Marsch, pp. 45-133, Springer-Verlag, New York.

McComas, D.J., S.J. Bame, P. Barker, W.C. Feldman, J.L. Phillips, P. Riley and J.W. Griffee (1998), Solar wind electron proton alpha monitor (SWEPAM) for the advanced composition explorer, *Space Sci. Revs.,86*, 563.

Messmer, P. (2002), Temperature isotropization in solar flare plasmas due to the electron firehose instability, *Astron. Astrophys., 382*, 301.

Ogilvie, K.W., L.F. Burlaga, D.J. Chronay and R. Fitzenreiter (1999), Sources of the solar wind electron strahl in 1995, *J. Geophys. Res., 104(A10)*, 22389-22393.

Ogilvie, K.W., R. Fitzenreiter and M. Desch (2000), Electrons in the low-density solar wind, *J. Geophys. Res., 105(A12)*, 27277-27288.

Paesold, G., and A. O. Benz (1999), Electron firehose instability and acceleration of electrons in solar flares, *Astron. Astrophys., 351*, 741.

Pagel, C., N. U. Crooker, D. E. Larson, S. W. Kahler, and M. J. Owens (2005), Understanding electron heat flux signatures in the solar wind, *J. Geophys. Res., 110*, A01103,

doi:10.1029/2004JA010767.

Phillips, J. L., and J. T. Gosling (1990), Radial evolution of solar wind thermal electron distributions due to expansion and collisions, *J. Geophys. Res., 95*, 4217, 1990.

Phillips, J. L., J. T. Gosling, D. J. McComas, S. J. Bame, and E. J. Smith (1989), ISEE 3 observations of solar wind thermal electrons with $T_\perp > T_\parallel$, *J. Geophys. Res., 94*, 13,377.

Pilipp, W. G., H. Miggenrieder, M. D. Montgomery, K.-H. Mühlhäuser, H. Rosenbauer, and R. Schwenn (1987a), Characteristics of electron velocity distribution functions in the solar wind derived from the Helios plasma experiment, *J. Geophys. Res., 92*, 1075.

Pilipp, W. G., H. Miggenrieder, K.-H. Mühlhäuser, H. Rosenbauer, R. Schwenn, and F. M. Neubauer (1987b), Variations of electron distribution functions in the solar wind, *J. Geophys. Res., 92*, 1103.

Rosenbauer, H., R. Schwenn, E. Marsch, B. Meyer, H. Miggenrieder, M. D. Montgomery, K. H. Mühlhäuser, W. Pilipp, W. Voges, and S. M. Zink (1977), A survey on initial results of the Helios plasma experiment, *J. Geophys. Res.*, *42*, 561.

Salem, C., D. Hubert, C. Lacombe, S. D. Bale, A. Mangeney, D. E. Larson, and R. P. Lin (2003), Electron properties and Coulomb collisions in the solar wind at 1 AU: Wind observations, *Astrophys. J.,* , *585*, 1147.

Scime, E. E., S. J. Bame, W. C. Feldman, S. P. Gary, and J. L. Phillips (1994), Regulation of the solar wind electron heat flux from 1 to 5 AU: Ulysses observations, *J. Geophys. Res., 99*, 23,401.

Scime, E. E., Littleton, J. E., S. P. Gary, Skoug, R., and Lin, N. (2001), Solar cycle variations in the electron heat flux: Ulysses observations, *Geophys. Res. Lett., 28*, 2169.

Sittler, E. C., Jr., and L. F. Burlaga (1998), Electron temperatures within magnetic clouds between 2 and 4 AU: Voyager 2 observations, *J. Geophys. Res., 103*, 17,447.

Smith, C.W., M. H. Acuna, L. F. Burlaga, J. L'Heureux, N. F. Ness and J. Scheifele (1998), The ACE Magnetic Field Experiment, *Space Science Reviews*, *86*, 613-632.

Smith, C.W., D.J. Mullan, N.F. Ness, R.M. Skoug and J. Steinberg (2001), Day the solar wind almost disappeared: Magnetic field fluctuations, wave refraction and dissipation, *J. Geophys. Res., 106*, 18625.

Stawicki, O., S. P. Gary, and H. Li (2001), Solar wind magnetic fluctuation spectra: Dispersion versus damping, *J. Geophys. Res., 106*, 8273.

Vocks, C., and G. Mann (2003), Generation of suprathermal electrons by resonant wave-particle interaction in the solar corona and wind, *Astrophys. J.,* , *593*, 1134.

Vocks, C., C. Salem, R. P. Lin, and G. Mann (2005), Electron halo and strahl formation in the solar wind by resonant interaction with whistler waves, *Astrophys. J.,* , *627*, 540.

Zurbuchen, T.H., S. Hefti, L.A. Fisk, G. Gloeckler, N.A. Schwadron, C.W. Smith, N.F. Ness, R.M. Skoug, D.J. McComas and L.F. Burlaga, (2001) On the origin of microscale magnetic holes in the solar wind, *J. Geophys. Res.*, *106(A8)*, 16001-16010.

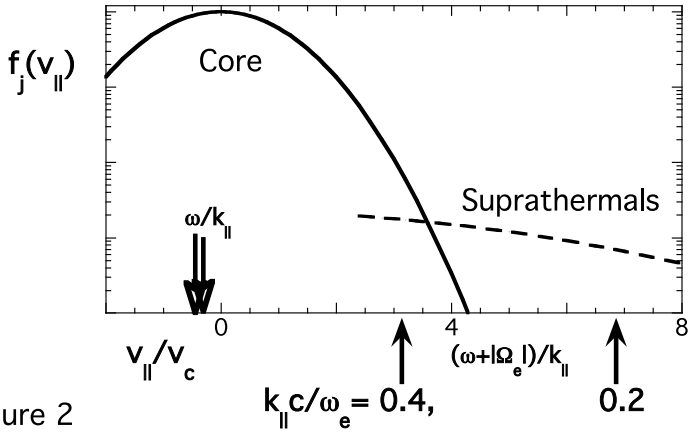

Figure 1. A cartoon illustrating the relationship among the reduced electron velocity distribution and two properties of left traveling whistler fluctuations at $k_{\|}c/\omega_e = 0.20$ and 0.40. The downward pointing arrows indicate the phase speeds ($\omega_r/k_{\|}$), whereas the upward pointing arrows denote the electron cyclotron resonance speeds $(\omega_r + |\Omega_e|)/k_{\|}$.

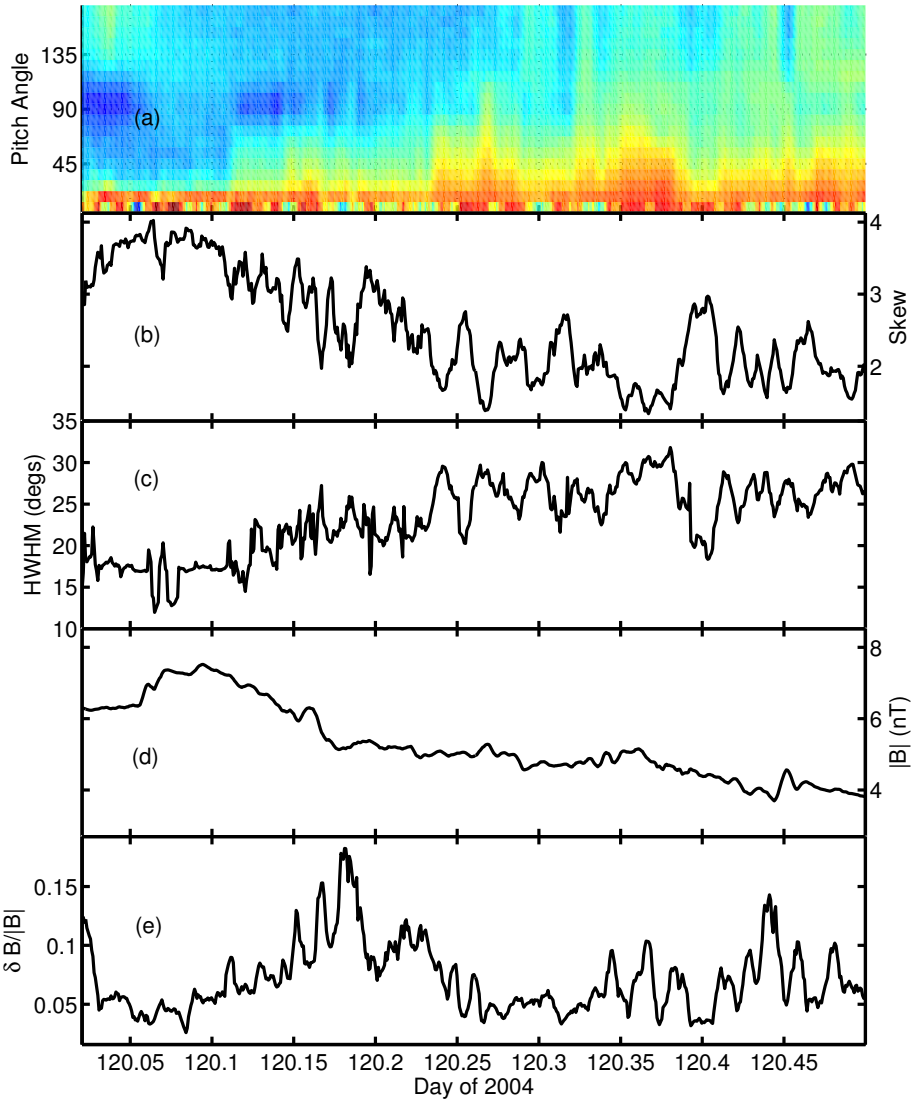

Figure 2. ACE/SWEPAM observations. Half a day of solar wind electron data. (a) electron pitch angle distributions at E=272eV. Colour represents log flux per pitch angle bin. (b) the skew of the pitch angle distribution. (c) Half width half maximum (HWHM) of the pitch-angle distributions fitted using a Gaussian over 90 degrees. (d) magnetic field strength and (e) RMS fluctuations $|\delta B|/B_o$.

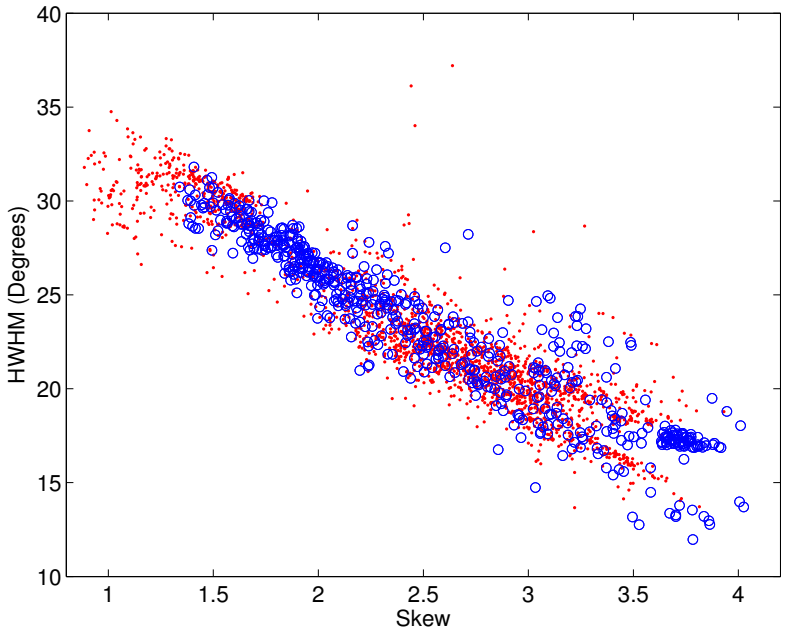

Figure 3. ACE/SWEPAM observations of suprathermal electrons. Scatter plots of skew vs HWHM over 2 time periods: days 120-120.5 (blue circles) and 86-87.5 (red dots) of 2004.

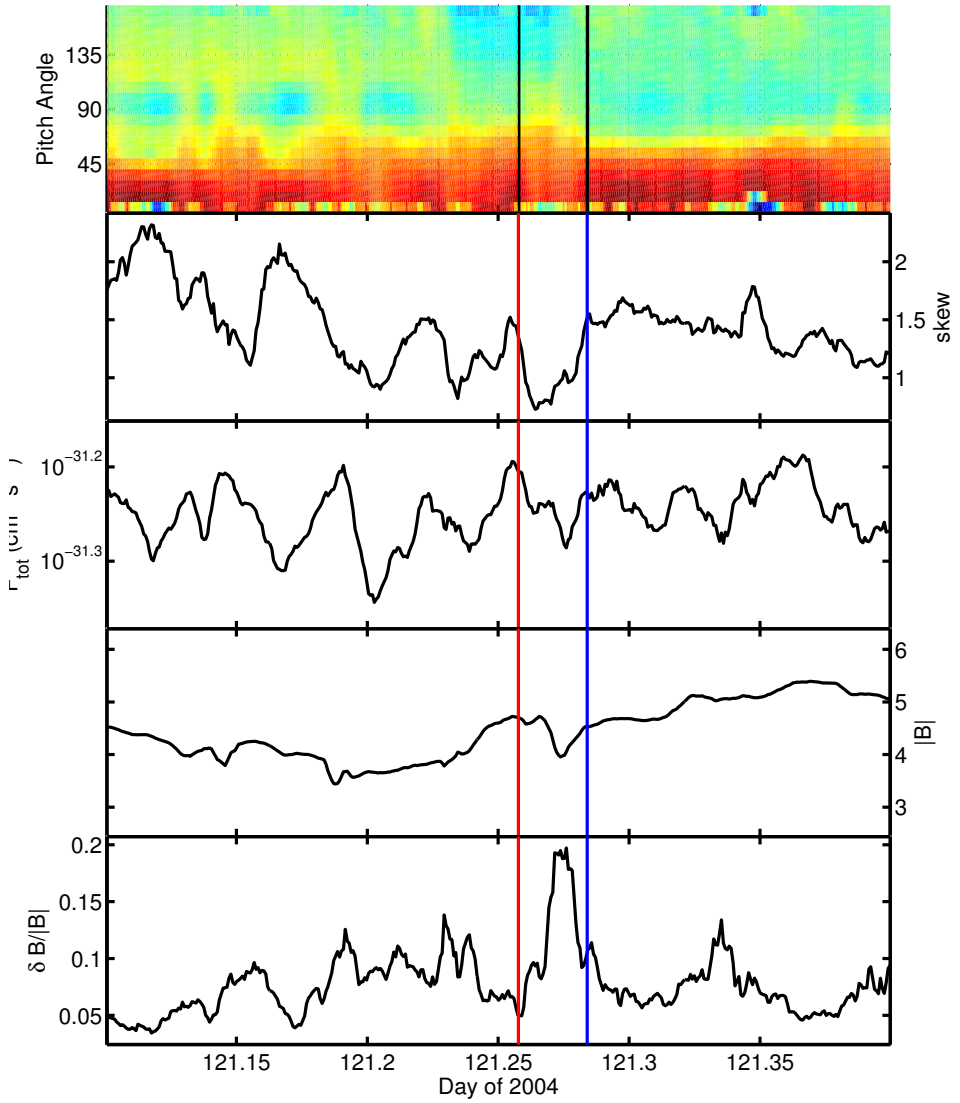

Figure 4. ACE/SWEPAM observations. An example event in 2004 for electrons at energy 519 eV. There is a broadening of the strahl and a clear drop in the skew during the interval of enhanced $|\delta B|/B_o$ which is bounded by the two vertical lines.

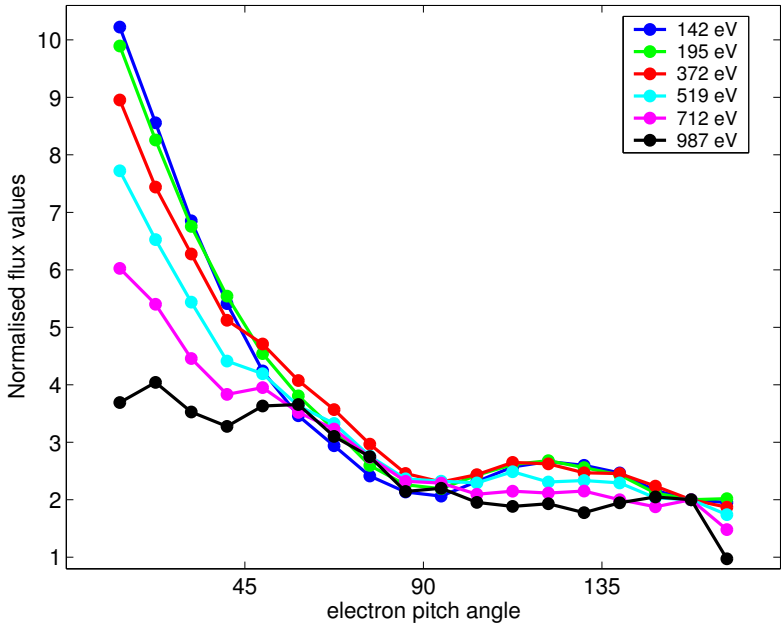

Figure 5. ACE/SWEPAM observations. Suprathermal electron pitch angle distributions for each energy averaged over the event beginning at DOY 86.9679 and ending on DOY 86.9809. The fluxes at each energy have been normalised to a value in the halo for better comparison. Pitch angle distribution widths clearly increase with increasing energy.

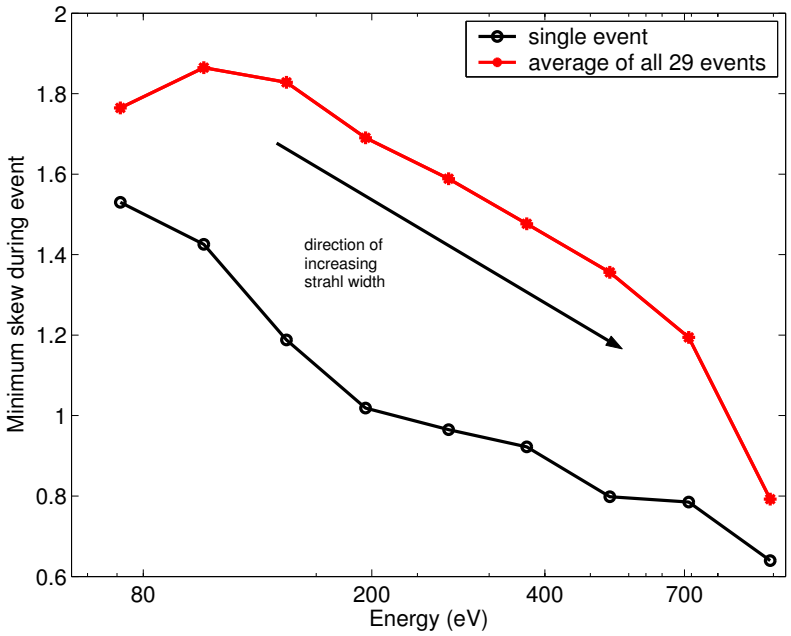

Figure 6. ACE/SWEPAM observations. Minimum skew of suprathermal electrons as a function of energy. The black line shows the result from the single event shown in Figure 5, while the red line gives the average minimum skew over all 29 events. For both cases a decreasing skew with increasing energy is clear.

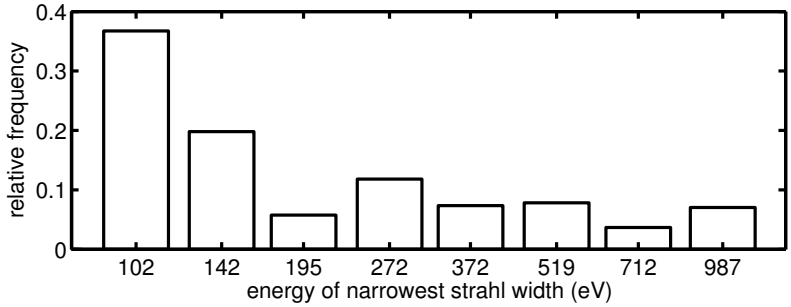

Figure 7. ACE/SWEPAM observations. Distributions of energies at which the strahl is narrowest for all 626 data points which comprise our 29 scattering events.

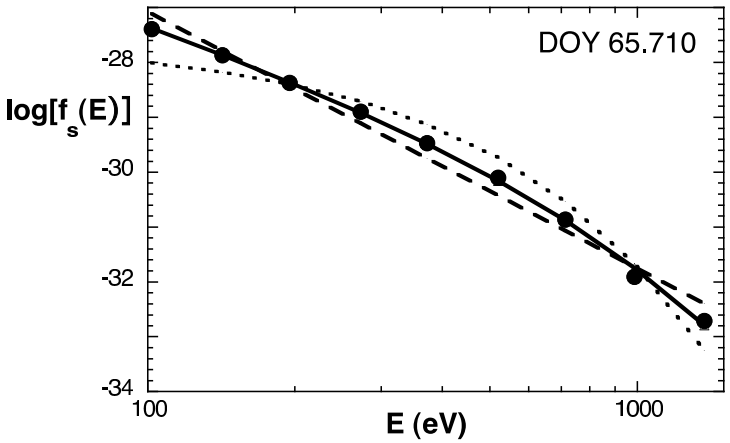

Figure 8. ACE/SWEPAM observations. The dots represent measurements of the strahl distribution at DOY 65.710. The dotted line represents an exponential fit to the observations using Equation (5) with $\gamma = 0$; the dashed line represents a power-law fit to the observations using Equation (5) with $\beta = 0$; and the solid line represents a full fit to Equation (5) with fitting parameters $ln(\alpha)$ = -21.2, γ = 1.29, and β = 0.00163.

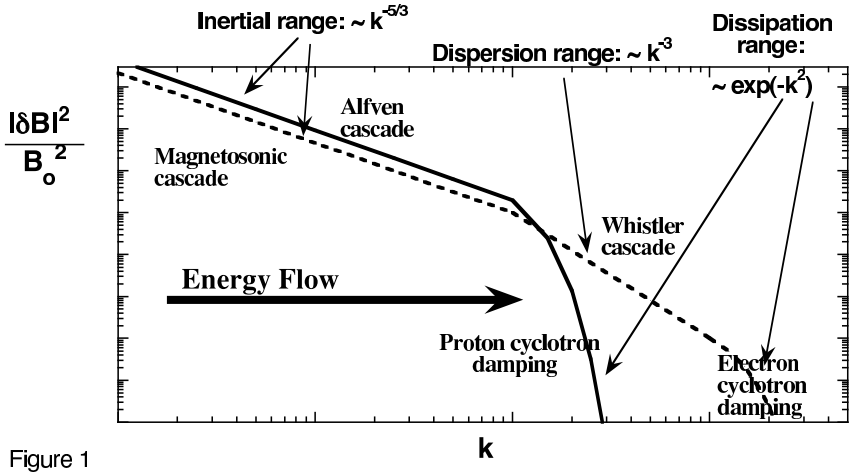

Figure 9. A cartoon illustrating a representative solar wind magnetic fluctuation power spectrum as a function of wavenumber